

CONTROL AND OPERATION OF A WIDEBAND RF SYSTEM IN CERN'S PS BOOSTER

M. E. Angoletta[†], S. Albright, A. Findlay, M. Haase, M. Jaussi, J. C. Molendijk, M. M. Paoluzzi, J. Sanchez-Quesada, CERN Geneva, Switzerland

Abstract

A prototype wideband High-Level RF (HLRF) system based on Finemet metal alloy has been installed in CERN's PS Booster (PSB) Ring 4 in 2012, within the frame of the LHC Injectors Upgrade (LIU) project. A digital Low-Level RF (LLRF) system was used to control the HLRF system to ascertain the capabilities of the combined system, especially under heavy beam loading.

The testing campaign was satisfactory and in 2015 the CERN management decided to replace all ferrite-based systems with Finemet ones for the PS Booster restart in 2020. This paper describes the LLRF features implemented for operating the wideband HLRF system and the main beam results obtained. Hints on the LLRF evolution in view of the PSB HLRF renovation are also given.

INTRODUCTION

A prototype wideband High-Level RF (HLRF) system based on Finemet Metal Alloy (MA) was installed in CERN's PS Booster (PSB) Ring 4 in 2012 [1], within the framework of the LHC Injectors Upgrade (LIU) project [2]. A digital Low-Level RF (LLRF) was used to control the wideband HLRF to ascertain the capabilities of the combined systems, especially under heavy beam loading. Initial tests not described here were carried out with a prototype LLRF system [3]. More advanced tests as well as beam operation were carried out in the 2014-2016 proton runs by using the new LLRF system deployed in the PSB in 2014 [4]. The positive outcome of these tests resulted in the decision to replace all ferrite-based HLRF systems with Finemet ones for the 2020 PS Booster restart.

LLRF SYSTEM OVERVIEW

The four PSB rings have been upgraded to a new, digital LLRF system in 2014, as described elsewhere [4]. The LLRF systems for PSB Rings 1..4 control the three, ferrite-based HLRF systems [5] installed in each ring and called C02, C04 and C16.

A fifth LLRF system called Ring 0 LLRF is installed as shown in Fig. 1. It can control the HLRF systems and beam in PSB Ring 4 for user-selectable cycles as a replacement of the standard Ring 4 LLRF. The Ring 0 LLRF is a hardware and software-upgraded version of the operational LLRF system, which can additionally control the wideband HLRF. Figure 2 shows the Ring 0 LLRF building blocks, their functions and input/output signals. Two additional boards interface to the wideband HLRF system. Additional input signals from this HLRF system are given to boards in the standard PSB LLRF ring con-

figuration to implement the various loops and to allow combined operation.

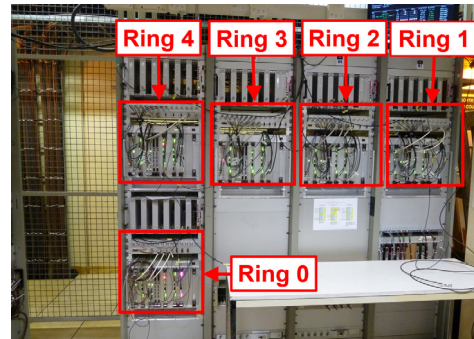


Figure 1: The five PSB LLRF systems.

System Capabilities

A customised Digital Signal Process (DSP) and front end software deployed in the Ring 0 LLRF provides the additional control features for parallel operation of ferrite and Finemet-based HLRF systems.

Board B receives gap return data at harmonic $h=1$ from the wideband HLRF system via an internal gigabit data link. This allows implementing the beam phase loop when the wideband system provides the accelerating voltage. Board C acquires the wideband gap return to implement the C04 phase loop with reference to the wideband cavities when required. Sophisticated and frequency-dependent rotation capabilities applied to the $h=1$ and $h=2$ wideband HLRF drive signal allow them to be aligned to their ferrite counterparts over the whole magnetic cycle for combined operation. The additional features are fully integrated within the controls infrastructure; full diagnostics and archiving capabilities are available.

Interface with HLRF

The wideband HLRF system is short-circuited by mechanical gap relays for cycles when it is not operated, so that its impedance does not perturb the beam. A dedicated, custom module (Cavity Control Interface) automatically removes the drive to the HLRF system if it drops. Four harmonics are servoed in voltage and in phase by the LLRF by using Cartesian [I,Q] coordinates. The gap return at four additional harmonics can be observed but no control capabilities are yet available. The 7.2 kV maximum voltage available from the wideband HLRF is slightly lower than the 8 kV provided by the C02 and C04 systems.

The control/acquisition power chain is adjusted to have sufficient regulation room available even when the HLRF amplifier gain collapses near full power. The LLRF limits the voltage requests and the cavity drive so as not to overdrive the HLRF.

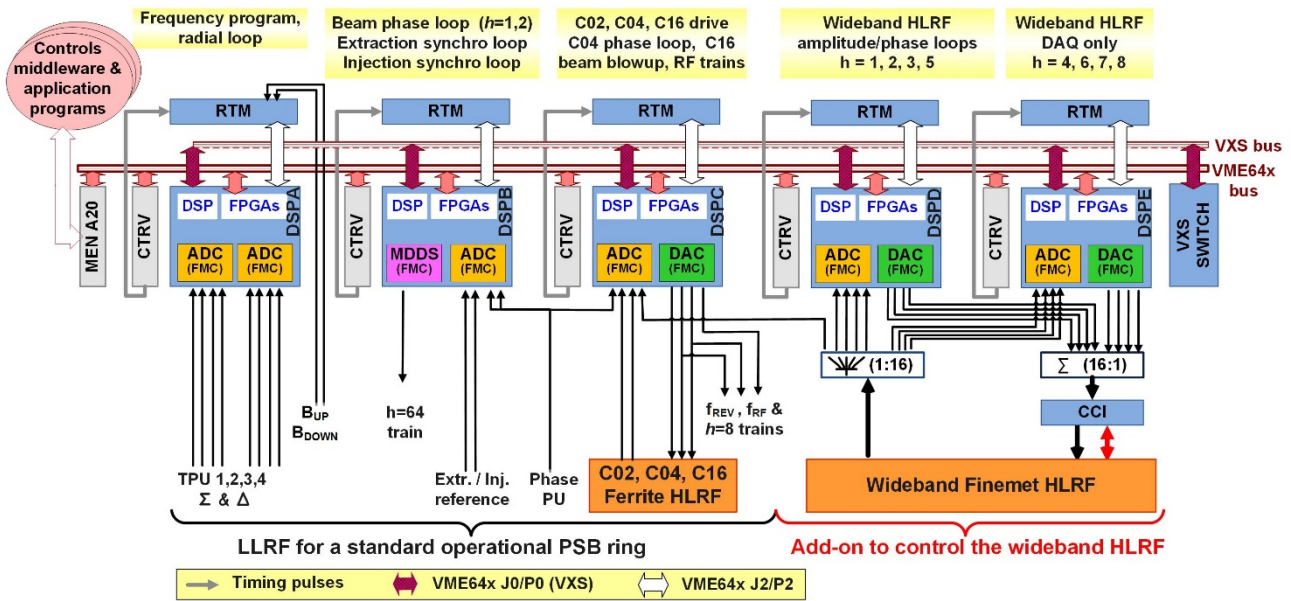


Figure 2: Ring 0 LLRF system. Keys: MDDS – Master Direct Digital Synthesiser; ADC – Analogue-to-Digital Converter; DAC – Digital-to-Analogue Converter; TPU – Transverse Pick-up; CTRV – Timing Receiver Module; MEN A20 – Master VME board; RTM – Rear Transition Module; CCI – Cavity Control Interface.

Beam Loading and Servoloops Effectiveness

The beam loading induced by a 730 E10 protons beam was measured by the LLRF at the first 6 harmonics during a whole PSB cycle, as shown in Fig. 3. The observed beam loading was higher at harmonics $h = 1,2,3,5$ thus the four servoloops available were set at these harmonics.

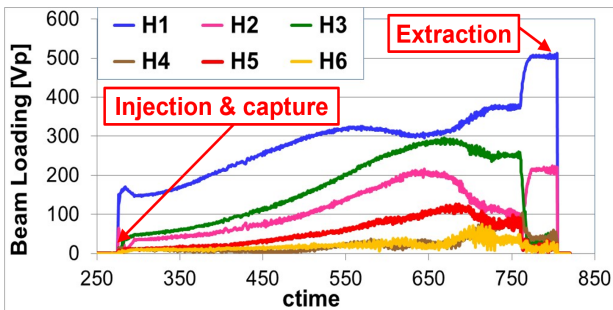


Figure 3: Voltage induced in the wideband HLRF by a 730 E10 protons beam and detected (with servoloops disabled) by the LLRF at $h = 1..6$.

The LLRF servoloops gain was evaluated by exciting the HLRF system via a Network Analyser (NA) sweeping the band around each of the four controlled harmonics. The reference for each servoloop was set to 0 V thus forcing a reduction of the induced voltage at these harmonics. The system was operated at a fixed frequency of 0.5 MHz, 1 MHz, and 1.5 MHz. The gap return signal was applied to the NA input and the normalised transfer function measured, as shown in Fig. 4. The achieved loop gain was of ~ 36 dB independently on the operation frequency. The loop gain was still of 10 dB at a frequency 2 kHz far from the main harmonics, where 2 kHz corresponds to the maximum synchrotron frequency for PSB beams. The measured loop bandwidth was of ~ 8 kHz,

which was confirmed by further step response measurements not shown here.

The LLRF loops performance satisfies the current PSB operation and is dominated by the $10 \mu s$ loop delay due to the DSP operation. Future planned improvements include the implementation of the servoloops on the on-board Field Programmable Gate Array (FPGA) chip, thus reducing the total delay to that given by cables (about $1 \mu s$) and increasing the loop bandwidth by a factor 10.

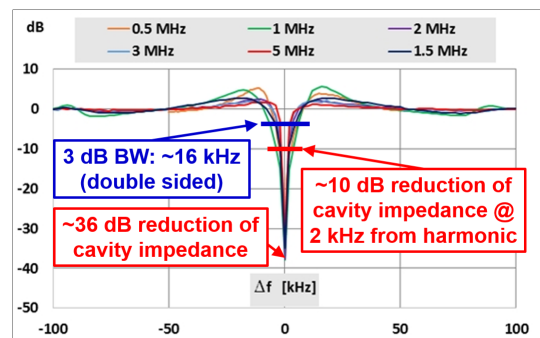


Figure 4: LLRF servoloops gain: normalised NA response.

LLRF OPERATION AND BEAM RESULTS

Achieving the operational characteristics for PSB beams require the use of all three HLRF ferrite-based systems: C02 for acceleration, C04 for shaping and splitting and C16 for longitudinal beam blowup.

The suitability of the combined LLRF/wideband HLRF systems for PSB operation was evaluated by implementing with the wideband HLRF system selected ferrite-based HLRF functions. The results obtained proved that the beam characteristics achieved by using the wideband HLRF fully matched those of the operational beams. A selection of unpublished beam results is provided below.

Other results showing the wideband system operating at $h=1$ (replacing the C02), at $h=2$ (replacing the C04) and as multi-harmonic at $h=1+2$ are available elsewhere [6].

Operation of Wideband HLRF for Beam Blowup

The wideband HLRF was controlled to replace the C16 HLRF system for longitudinal emittance blowup. The LLRF phase modulation capabilities used for C16 operation were applied to the wideband cavity drive signal. Contrary to the C16 case, a fixed harmonic could be kept for the wideband system, as its operational range covered the whole PSB cycle. The three main PSB blowup operational modes were successfully reproduced.

First, the longitudinal emittance was increased for an *ISOLDE* beam with maximum intensity. A longitudinal blowup from the initial 1.75eVs to 3.3eVs for 900 E10 protons was successfully achieved.

Secondly, the *LHC25ns* beam specifications of 1.3eVs for 165 E10 particles were matched with excellent particle distribution. The maximum blow up of 2.5 eVs required by the large emittance beam studies was also achieved.

Finally, the *LHCINDIV* beam was successfully delivered. The HLRF voltage controlled its intensity in the 2-12·E10 protons range by increasing the longitudinal emittance prior to shaving. The C16 performance was matched and the beam intensity with a constant emittance at extraction of 0.3 eVs was adjusted via the wideband HLRF voltage. Figure 5 shows two tomograms with intensity of 2 E10 (left) and 12 E10 protons (right).

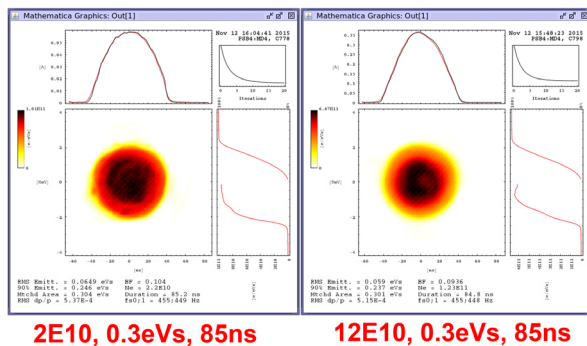


Figure 5: *LHCINDIV* beam tomograms: 2 E10 (left) vs 12E10 protons (right) for the same 0.3 eVs emittance.

Operation of Wideband HLRF at $h=3$

The wideband HLRF was used to add a novel $h=3$ voltage contribution to the standard $h=1+2$ operation in bunch-lengthening mode obtained by the combined C02 and C04 HLRF systems. The expectation was to mitigate the space charge limitations by further reducing the longitudinal line density thus minimising the losses, especially at capture.

The Ring 0 LLRF was upgraded in 2016 to implement additional voltage and phase programs at $h=3$. A total voltage of 16 kV was split over the C02, C04 and $h=3$ wideband systems in a 2:2:1 ratio, i.e. 6.4 kV on the C02 and C04 systems and 3.2 kV on the wideband system at $h=3$. The beam intensity behaviour over the PSB cycle

was compared with that of the standard $h=1+2$ operation when the 16 kV total voltage was equally split between C02 and C04 systems. Preliminary results [7] shown in Fig. 6 suggest that the three-harmonics operation allows keeping a higher intensity than the standard double-harmonic operation. Further studies are planned for the 2017 run.

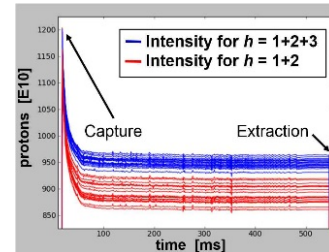


Figure 6: PSB cycle intensity for double (red) and triple (blue) harmonic operation and 16 kV total HLRF voltage.

Reliability Runs

Two reliability runs were carried out in 2015 and 2016, where the combined Ring 0 LLRF and wideband HLRF provided high-intensity operational beam to the *ISOLDE* experimental facility. The wideband HLRF successfully replaced the C04 system; standard beam characteristics were reliably matched. The voltages used were of 8 kV on the C02, 7.2 kV on the wideband HLRF at $h=2$, and 600 V on the C16 systems. The $h=2$ wideband drive signal phase was programmed to provide shaping capabilities.

The 2015 reliability run lasted 2 months and was very successful. The 2016 reliability run was stopped after 10 days of operation for water cooling problems in the wideband HLRF prototype power amplifier. Corrective measures have been taken and a new reliability run is planned for 2017. No problems with the LLRF control and operation emerged during both these runs.

CONCLUSIONS AND OUTLOOK

The Ring 0 LLRF system has proven its effectiveness and reliability in successfully controlling the wideband HLRF for operation and for studies in the 2014-2016 PSB runs. Novel features, such as the $h=3$ operation, have also been added and will be further exploited in the coming run.

A heavy developments and studies program is planned for the 2017-18 PSB runs. A new, fixed frequency clocking scheme [8] will be deployed in the Ring 0 LLRF, similarly to what is used elsewhere [9]. A novel longitudinal emittance blowup scheme using band limited phase noise at the accelerating harmonic [10] and planned for the PSB operational rings [4] will be deployed for the wideband HLRF system, too. The servoloops will be implemented in the FPGA to achieve higher loop bandwidth; methods to deal with more than one harmonic per hardware channel will be validated. Data on combined HLRF-LLRF behaviour will be collected for simulations [11]. Finally, the experience gathered in other machines equipped with the same LLRF and more than one wideband HLRF systems [12] will be useful to define the new PSB LLRF features.

ACKNOWLEDGMENTS

The long lasting collaboration between CERN, KEK and J-PARC on wideband, MA loaded cavities studies as well as the various Japanese contributions (MA cores, amplifiers, radiation testing, etc.) played a very important role for this project. They have been sincerely appreciated and are gratefully acknowledged.

REFERENCES

- [1] M. M. Paoluzzi et al. “Design of the New Wideband RF System for the CERN PS Booster”, in *Proc. IPAC '16*, Busan. Korea, May 2016, pp. 441-443.
- [2] K. Hanke et al., “The LHC Injectors Upgrade (LIU) Project at CERN: Proton Injector Chain”, presented at IPAC'17, Copenhagen, May 2017, paper WEPVA036.
- [3] M. E. Angoletta et al., “CERN’s PS Booster LLRF Renovation: Plans and Initial Beam Tests”, in *Proc. IPAC '10*, Kyoto, Japan, May 2010, pp. 1461-1463.
- [4] M. E. Angoletta et al., “Operational Experience with the New Digital Low-Level RF System for CERN’s PS Booster”, presented at IPAC'17, Copenhagen, May 2017, paper THPAB143.
- [5] A. Krusche et al., “The New Low-Frequency Accelerating Systems for the CERN PS Booster”, in *Proc. EPAC '98*, Stockholm, Sweden, June 1998, p. 1782.
- [6] M. M. Paoluzzi et al., “Beam Tests Using a Wide Band RF System Prototype in the CERN PS Booster”, in *Proc. IPAC '15*, Richmond, Virginia, May 2015, pp. 3134-3137.
- [7] S. Albright, M.E Angoletta, E. Benedetto, M. Jaussi, “RF Capture in a Triple Harmonic Bucket”, unpublished.
- [8] J. C. Molendijk, “Fixed frequency clock Digital LLRF modulator and demodulator scheme for seamless wide RF frequency coverage”, unpublished.
- [9] M.E. Angoletta et al, “Initial Beam Results of CERN ELENA’s Digital Low-Level RF System”, presented at IPAC'17, Copenhagen, May 2017, paper THPAB142.
- [10] D. Quartullo, E. Shaposhnikova, H. Timko, “Controlled Longitudinal Emittance Blow-up Using Band-Limited Phase Noise in CERN PSB”, presented at IPAC'17, Copenhagen, May 2017, paper THPVA024.
- [11] D. Quartullo, S. Albright, E. Shaposhnikova, “Studies of Longitudinal Beam Stability in CERN PS Booster After Upgrade”, presented at IPAC'17, Copenhagen, May 2017, paper THPVA023.
- [12] M. E. Angoletta et al., “CERN’s LEIR Digital LLRF: System Overview and Operational Experience”, in *Proc. IPAC '10*, Kyoto, Japan, May 2010, pp. 1464-1466.